Catalysis Science & Technology

Accepted Manuscript

ROYAL SOCIETY OF CHEMISTRY

www.rsc.org/catalysis

Journal Name

RSCPublishing

ARTICLE

Rapid Degradation of Oxidation Resistant Nitrophenols by TAML Activator and H_2O_2

Cite this: DOI: 10.1039/x0xx00000x

Received ooth January 2012,
Accepted ooth January 2012

DOI: 10.1039/x0xx00000x

www.rsc.org/

Soumen Kundu,† Arani Chanda,† Jasper V. K. Thompson, George Diabes, Sushil K. Khetan, Alexander D. Ryabov*, and Terrence J. Collins*

Nitrophenols (NPs) are widely prevalent recalcitrant anthropogenic pollutants. TAML activators in conjunction with peroxides have proven to be effective in the remediation of myriad organic pollutants. In the present study, we have discovered that one of the most reactive TAML activators $[Fe\{4,5\text{-}Cl_2C_6H_3\text{-}1,2\text{-}(NCOCMe_2NCO)_2CF_2\}(OH_2)]^-$ (**1**) catalyses the oxidative degradation by H_2O_2 of mono- and dinitrophenols (including all US-EPA classified priority pollutants) under ambient conditions at pH 8 which is close to pH of environmental waters. Individual nitrophenols as well as mixtures thereof undergo fast decontamination (reaction time ≤45 min) resulting in deep oxidation producing HCO_2^- and minerals, CO, CO_2, NO_2^-, and NO_3^- (up to 99% of N and 70% of C). The remarkable efficacy of the **1**/H_2O_2-mediated decontamination process is matched by complete elimination of the toxicity of the nitrophenols (Microtox® assays). Detailed mechanistic studies of the catalyzed oxidation revealed a strong substrate inhibition of the catalytic activity for some nitrophenols, the strongest being observed for 4-nitrophenol. DFT calculations suggest that the inhibition is likely due to reversible binding of nitrophenolate anions to the iron(III) center of the resting state of the **1** catalyst, which compromises its reactivity toward H_2O_2.

Introduction

Nitrophenols (NPs) are one of the most widely used chemicals in the herbicide, agrochemical, pharmaceutical, rubber, and munitions industries.[1, 2] The pesticides parathion, fluoridifen, and fenitrothion incorporate the NP unit. 2-Amino-5-nitrophenol and 2-amino-6-chloro-4-nitrophenol are used as colorants in hair dyes and in the production of azo dyes (Solvent Red 8, Eriochrome Black T). Dinitro-*o*-cresol is a potent herbicide.[3] 2-NP is a high production volume (HPV) chemical exceeding one million pounds per annum in the United States.[4] Di-*tert*-butylnitrophenol, formed by the nitration of an antioxidant present in turbine lubricating oil, is a submarine contaminant.[5] Due to the extensive use, NPs are a major class of anthropogenic pollutants which enter water streams primarily as run-off from industrial waste.[1, 6] 2-NP, 4-NP, 2,4-dinitrophenol, and 4,6-dinitro-*o*-cresol have been classified as priority pollutants by the United States Environmental Protection Agency.[7] Nitrophenols are stable, water soluble, environmentally persistent, and toxic to many life forms.[1, 8] Slow biodegradation and bioaccumulation mark these compounds that remain active in the environment for long periods.[1, 2, 6] 2-NP is carcinogenic and 4-NP is an endocrine disruptor showing estrogenic and anti-androgenic activities in vivo.[9]

Due to numerous environmental problems associated with NPs, several remediation technologies have been developed. The more promising include direct photolysis by UV light,[6] photo-catalytic degradation by TiO_2[2, 10, 11] and a carbon nanotube/TiO_2 composite catalyst,[11] laser flash photolysis,[6] microbial fuel cell assisted photo-catalytic oxidation,[10] treatment with O_3,[12] Fenton and photo-Fenton processes,[8] microbial degradation.[1] Although the processes degrade NPs, many have distinct limitations. For example, the biological treatment of contaminated hot-spots is slow and leaves other toxic compounds in the mix. Effective biodegradation requires adequate supplies of nutrients, optimal pH and temperature, and eventual disposal of the activated sludge.[2, 13] Photochemical processes need special reactors and long reaction times (>12 h for 1×10^{-4} M 4-NP).[6] Fenton chemistry is typically run at acidic pHs (2–3) with high loadings of iron salts.[14] The iron containing sludge generated by the process can lead to unwanted growth of algae. Thus, the current technologies for remediating NPs are far from ideal limiting real-world efficacy.

TAML activators (**1**, Figure 1) have demonstrated high performance in the degradation of recalcitrant pollutants in water.[15-17] We have previously reported on the **1**/H_2O_2 catalyzed total degradation of pesticides Fenitrothion and Parathion, which contain the 4-NP unit.[18] 2,4,6-Trinitrotoluene (TNT) and 1,3,5-trinitrobenzene (TNB) are also oxidatively degraded by **1**/peroxide in micellar aqueous media through the intermediate formation of Meisenheimer complexes.[19] Here we demonstrate the efficacy of **1**/H_2O_2 system in the oxidative degradation of six mononitrophenols (MNPs) and four dinitrophenols (DNPs) as shown in Figure 1. All these priority NP pollutants are rapidly (3–45 min) and deeply degraded under ambient conditions at pH 8. The fast oxidation of individual NPs and their mixtures affords nitrogen and carbon minerals with elimination of toxicity in bacterial assays.

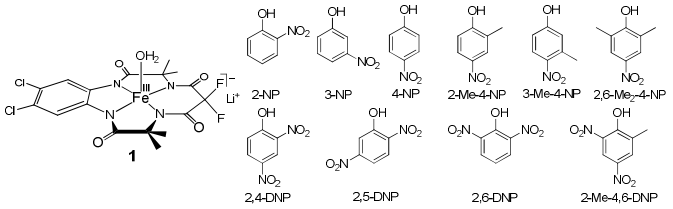

Figure 1. Structures of TAML activator (**1**), mono- and dinitrophenols used in this work: 2-nitrophenol, 2-NP; 3-nitrophenol, 3-NP; 4-nitrophenol, 4-NP; 2-methyl-4-nitrophenol, 2-Me-4-NP; 3-methyl-4-nitrophenol, 3-Me-4-NP; 2,6-dimethyl-4-nitrophenol, 2,6-Me_2-4-NP) and dinitrophenols (2,4-dinitrophenol, 2,4-DNP; 2,5-dinitrophenol, 2,5-DNP; 2,6-dinitrophenol, 2,6-DNP; 2-methyl-4,6-dinitrophenol, 2-Me-4,6-DNP.

Experimental Section

Materials and Methods

Catalyst **1** (Figure 1) was synthesized as previously described[20] and purified by column chromatography using C-18 reverse phase silica gel and a gradient water/methanol mobile phase. Reagent grade H_2O_2 (30% w/w) was purchased from Fluka. H_2O_2 solutions were standardized spectrophotometrically daily (extinction coefficient 72.4 M^{-1} cm^{-1} at 230 nm[21]). Catalase (from *Aspergillus niger*, 2350 U mg^{-1}) was obtained from Sigma-Aldrich. Nitrophenols (MNP and DNP) of the highest available purity were purchased from commercial sources (Sigma-Aldrich, Fluka, Fisher, Acros) and further purified by recrystallization from ethanol/water mixture according to established procedures.[22] *tert*-Butanol (99.5%) was purchased from Aldrich. HPLC grade methanol, ethanol, and water were purchased from Fischer. An aqueous solution of NaOH (Aldrich) was used for pH adjustment of buffered solutions. Ion chromatography standards for nitrate (1000 mg L^{-1}) and nitrite (1000 mg L^{-1}) were purchased from Fluka Analytical and formate (1001 µg mL^{-1}) was purchased from Alltech.

Methods

Kinetic measurements were performed at 25 °C using an Agilent spectrophotometer (model 8453) equipped with a thermostated cell holder and an automatic 8-cell positioner. The pH measurements were performed using a Corning 220 pH meter calibrated with standard buffer solutions at pHs 4, 7, and 10. The degradations of NPs were followed by HPLC (Supporting Information, SI). The end products of NP degradation were quantified using ion chromatography (see the SI). Total organic carbon (TOC) analyses were performed by Analytical Laboratory Services, Inc. Middletown, PA (USA) to determine the extent of mineralization during degradation. The reaction mixture was adjusted to pH 2 by addition of HCl (~6 M). Aquatic toxicity studies of the starting NPs and final degradation mixture employed *Vibrio fisheri* Microtox® assays and were performed at Coastal Bioanalysts Inc., Gloucester, VA (USA). The degradation reaction mixture was quenched with catalase and the pH of the solution was adjusted to neutral (pH ~7) for these studies.

Stock solutions of nitrophenols (2×10^{-3} M) were prepared in a *tert*-butanol/water (3:7) mixture. *tert*-Butanol was used to increase the solubility of NPs. In a typical experiment, appropriate volumes of buffer of desired pH, NP and **1** stock solution were added in the reaction vial to attain the desired molar concentrations. The reaction was initiated by the addition of the appropriate volume of H_2O_2. UV-vis experiments were performed in disposable polystyrene cuvettes. For TOC analyses, use of *tert*-butanol was avoided, as it interferes with accurate measurement of organic carbon from NPs. In these cases, dilute stock solutions of NPs (2×10^{-4} M) were prepared in buffered aqueous solution (pH 8, 0.1 M phosphate).

Density functional theory (DFT) calculations were carried out using Becke's three parameter hybrid functional (B3LYP) and basis set 6-31G provided by the Gaussian 03 (release D.01) software package. The geometry optimization for complex **1** with 4-NP were terminated upon reaching the default convergence criteria. The optimizations did not impose any symmetry. Geometry optimizations for each species were performed in absence of a solvent (in vacuum) and then a single point calculation was performed in water (ε = 78.3) using polarizable continuum model (PCM).

Results and Discussion

Oxidative Degradation of Nitrophenols: Optimized Conditions, End Product Quantification, and Toxicity Studies

Optimization of Reaction Conditions and Determination of End Products

Addition of **1**/H_2O_2 to the aqueous solutions of nitrophenols resulted in the fast disappearance of the yellow color characteristic of nitrophenolates with a concomitant absorbance decay around 400 nm as monitored by UV-vis spectroscopy. The reactivity of **1** and other TAML activators is pH dependent[23-25] and **1** exhibits maximal activity at pH 10,[15, 23, 25] which is typically too basic for environmental applications. Therefore, the experiments were performed at pH 8 which is close to environmental conditions and at which **1** has a longer lifetime under the operating conditions.[15] The conditions were

then optimized (Table 1) to achieve total degradation (≥99.5%, HPLC data) in less than 30 and 45 min for MNPs and DNPs, respectively, at pH 8 (0.1 M phosphate) using minimal loadings of **1** and H_2O_2. Each nitrophenol (1×10^{-4} M) required different amounts of **1** ($(0.2–4)\times10^{-6}$ M, Table 1), H_2O_2 ($(2–5)\times10^{-2}$ M, Table 2) for their complete removal (≥99.5%) over 3–45 min. The mixtures were quenched after complete removal of the parent NP (Table 1) and analyzed for mineralized nitrogen (IC analysis) and carbon (IC and TOC, see experimental section). The final reaction mixtures showed a significant release of nitrogen as nitrite and nitrate (72–99 % of total N, Table 1). The NP carbon was found as formate (0.96–7.17%, Table 1) and $CO+CO_2$ (16–63%, Table 1), both with respect to total C. Other small acids (oxalic, maleic, methyl maleic, glycolic) were not detected (IC studies), though they have been previously observed in oxidations of other organic pollutants by TAML/peroxide systems.[18, 26] Total mass balance for N and C could not be achieved which, as has been previously argued,[27, 28] is likely due to the presence of larger organic fragments that could not be positively identified. However, the release of nitrogen and carbon as minerals, the total (≥99.5%) removal of the parent NPs and the drastic reduction in toxicity (see below) are indicative of deep and effective oxidations of the NPs and the organic fragments produced. Multiple NPs often co-exist in pollution hot-spots and therefore NP mixtures were also treated with **1**/H_2O_2. Mixture of all six MNPs (1×10^{-4} M each, Figure 1S, see the SI) was treated with **1**/H_2O_2. The amounts of **1** (6.9×10^{-6} M) and H_2O_2 (1.8×10^{-1} M) corresponded with the optimal conditions determined for each individual NP (Table 1). All NPs in these mixtures were completely oxidized (≥99.5%) within 30 min (Figure 1S). Similarly, mixtures of four DNPs were completely destroyed (≥99.5%) within 45 min (Figure 2S, see the SI).

Toxicity Studies

The toxicity reduction consequent to treatment is an important marker of the environmental performance of the **1**/H_2O_2 system. Solutions of 3-NP and 4-NP (both 1×10^{-3} M) and other NPs (Table 2) were tested by Microtox® assays using the bioluminescent bacteria *Vibrio fisheri*. EC_{50} values represent the percentage of the test solution required to produce 50% mortality of the bacteria in 15 min time. Thus, a lower number is reflective of higher toxicity. Acute toxicity toward these microbes is typical for 3-NP and 4-NP which manifests the EC_{50} values of 13.1 and 35.1%, respectively. Treatment of solutions of 3-NP and 4-NP by **1**/H_2O_2 resulted in a drastic reduction of toxicity (Table 2). This can be seen because the treated solutions did not result in 50% reduction in the bacteria population in 15 min, which correlates with EC_{50} values of >100% (Table 2). Similar reduction of toxicity was also observed for multiple DNPs (Table 2) demonstrating that the treatment by **1**/H_2O_2 is extremely effective in mitigating the toxicity of NPs (as measured by Microtox® assay). Of course, these are rudimentary toxicity assays which do not capture information on developmental toxicity associated with endocrine disruption,[29] where such studies are beyond the scope of this work.

Table 1. Optimized conditions and quantified end products after the total (≥99.5%) degradation of mono- and dinitrophenols at pH 8 (0.1 M phosphate) and room temperature (see experimental section for details).

Substrate [a]	[**1**][b]	$[H_2O_2]$[c]	Time [d]	NO_2^- + NO_3^-(%)	HCO_2^- (%)	$CO+CO_2$ (%)
2-NP	2	40	30	87±0.6	3.2±0.1	20
3-NP	2	40	30	99±0.1	3.78±0.02	35
4-NP	1.3	40	20	99±0.5	7.17±0.07	63
2-Me-4-NP	0.6	20	9	73.0±6.3	2.89±0.01	24
3-Me-4-NP	0.8	20	15	85.0±0.8	4.17±0.03	35
2,6-Me_2-4-NP	0.2	20	3	98.0±1.4	0.96±0.05	–[e]
2,4-DNP[f]	4	50	45	75±1	2.1±0.1	46
2,5-DNP	1.8	40	40	82±2	2.5±0.8	35
2,6-DNP[g]	2.5	40	20	72±2	3.4±0.7	16
2-Me-4,6-DNP[h]	3	50	40	88.0±0.3	4.7±0.1	20

[a] [Nitrophenol] = 1×10^{-4} M; [b] In μM L^{-1}; [c] In mM L^{-1}; [d] In min; following disappearance of NP by HPLC; [e] could not be reliably measured. [f] **1** and H_2O_2 were added in two equal aliquots at $t = 0$ and $t = 25$ min; [g] **1** and H_2O_2 added at $t = 0$ and $t = 10$ min. [h] **1** and H_2O_2 added at $t = 0$ and $t = 20$ min.

Table 2 Aquatic toxicity studies with Microtox® assays for select nitrophenols and their **1**/H_2O_2 catalyzed degradation mixture.

Substrate	Initial Substrate (1 mM, EC_{50})	Final Reaction Mixture (EC_{50})
3-Nitrophenol	13.1% (18.1 μM)	>100% [a]
4-Nitrophenol	35.1% (48.4 μM)	>100% [b]
2,4-DNP	71.6% (131 μM)	>100% [c]
2,5-DNP	6.8% (12.4 μM)	>100% [c]
2,6-DNP	32.6% (59.6 μM)	92.2% [d]
2-Me-4,6-DNP	30.0% (59.1 μM)	>100% [c]

EC_{50} values reported are shown as percentage of testing solution required to produce 50% mortality of *Vibrio fisheri* in 15 min. Absolute values for pure compounds are also listed in parentheses [a] [3-NP] 1×10^{-3} M, [**1**] 1×10^{-5} M, $[H_2O_2]$ 4×10^{-1} M, [b] [4-NP] 1×10^{-3} M, [**1**] 1×10^{-5} M, $[H_2O_2]$ 2×10^{-1} M, [c] [DNP] 1×10^{-3} M, [**1**] 2×10^{-5} M, $[H_2O_2]$ 5×10^{-1} M, [d] [2,6-DNP] 1×10^{-3} M, [**1**] 2×10^{-5} M, $[H_2O_2]$ 8×10^{-1} M, pH 8, room temperature.

Kinetic, Mechanistic and DFT Studies of Nitrophenol Oxidation

TAML activators are small functional replicas of peroxidase and short-circuited cytochrome P450 enzymes.[25, 30] They are remarkably effective in the oxidative degradation of organic substrates containing phenolic moieties.[15, 16, 18, 19, 26] The

intimate mechanisms of action for this family of catalysts has been well deciphered (see below)[23, 25, 31-33] and this provided a tool for to advancing the conceptually based iterative design process[34, 35] aimed at more robust and reactive catalysts. Our mechanistic approach lends itself well to studying substrate oxidations and in this contribution we investigate the kinetic and mechanistic dimension of the decompositions of nitrophenols for the first time.

MONONITROPHENOL

The kinetic experiments performed in this work were planned based on the general mechanism of catalysis by TAML activators shown in Scheme 1.[26] TAML activator (Fe^{III}-TAML) is reversibly oxidized by H_2O_2 (k_1, k_{-1}) to form "Oxidized TAML" which then attacks targeted substrates (k_{II}). The nature of the "Oxidized TAML" depends on the pH which determines the equilibration between *aqua*, *hydroxo* and *oxo* complexes. Each of these have been kinetically implicated at the Fe^{IV} oxidation state[23] and a monooxo complex is now well established for the Fe^{V} state.[36, 37] Both the iron(IV) and iron(V) states are known to be oxidizing, the latter being the much more powerful oxidant, and kinetic evidence for both 1- and 2-electron processes has been obtained.[36] Under steady-state conditions, the reaction rate is expressed by eq (1), which was derived by applying the steady-state approximation to "Oxidized TAML" together with the mass balance equation $[Fe^{III}]_t = [Fe^{III}\text{-TAML}] + [\text{Oxidized TAML}]$. The rate constant k_{-I} in eq (1) is negligible compared to the term ($k_I[H_2O_2] + k_{II}[NP]$).[26] Equation 2 was obtained upon rearrangement of eq 1. The rate constant k_I should be independent of the nature of NP, whereas the value of k_{II} depends upon it. According to previous studies, k_I and k_{II} depend strongly upon pH, which originates from the Brønsted acidity of axial water ligands on iron[23, 25] and hydrogen peroxide.[25]

$$Fe^{III}\text{-TAML} + H_2O_2 \underset{k_{-I}}{\overset{k_I}{\rightleftharpoons}} \text{(Oxidized TAML)}$$

$$\text{(Oxidized TAML)} + \text{Nitrophenol} \xrightarrow{k_{II}} Fe^{III}\text{-TAML} + \text{Oxidized Nitrophenol}$$

$$\text{Oxidized Nitrophenol} \xrightarrow{fast} \text{Final Product(s)}$$

Scheme 1. General mechanism of catalysis by TAML activators.

$$Rate = \frac{k_I k_{II}[H_2O_2][NP][Fe^{III}]_t}{k_{-I} + k_I[H_2O_2] + k_{II}[NP]} \quad (1)$$

$$\frac{[Fe^{III}]_t}{Rate} = \frac{1}{k_I[H_2O_2]} + \frac{1}{k_{II}[NP]} \quad (2)$$

The rate constants k_I and k_{II} (Scheme 1) for the MNPs were determined at pH 8.4 (instead of pH 8 used for total oxidative degradation) to ensure that the concentrations of the nitrophenolates were at least 10 times that of the nitrophenols in accordance with the known pK_a values for the mononitrophenols (see Table 2S, see the SI).

The *initial rates* of NP oxidation were measured using UV-vis spectroscopy at 25 °C. A typical case is described here for the 4-NP oxidation. The reaction between, for example, 4-NP (1.1×10^{-4} M) and H_2O_2 (4.9×10^{-3} M) was initiated by the addition of peroxide to the solution of 4-NP and **1** (1.0×10^{-6} M). The corresponding spectral changes are shown in Figure 2. The initial rate was calculated from the slope of the linear plot (Inset to Figure 2) using the experimentally determined extinction coefficient of 4-NP at λ_{max} at pH 8.5 (ε_{401nm} =17500±200 M^{-1} cm^{-1}). The rate of non-catalytic oxidation of 4-NP by H_2O_2 in the absence of **1** (<5% of the catalyzed rate) was subtracted from the measured rate in the presence of **1**.

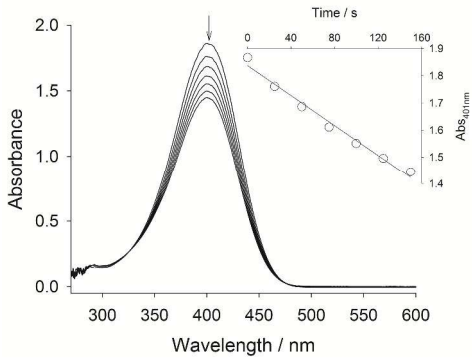

Figure 2. Spectral changes associated with the catalytic oxidation of 4-nitrophenol by **1**/H_2O_2. The arrow indicates a decrease in absorbance at 401 nm due to oxidation of 4-NP. Conditions: [**1**] 1.0×10^{-6} M, [H_2O_2] 4.9×10^{-3} M, [4-NP] 1.1×10^{-4} M, pH 8.4 (0.1 M phosphate), 25 °C. *Inset*: The decrease in absorbance at 401 nm as a function of time used for calculating the initial rate of oxidation. Data were collected every 5 s and plotted for every 25 s for clarity.

The initial rate for NP oxidation increased hyperbolically (for 3-Me-4-NP in Figure 3 and in most cases, see text) with increasing [H_2O_2] (Figure 3A) and [NP] (Figure 3B) and linearly (passing through the origin) with increasing [**1**] (Figure 4) as mandated by eq 2 and as observed for other organic substrates.[23, 26] Consistent with eq 2, the inverse initial rate was a linear function of the inverse of both [H_2O_2] (Inset to Figure 3A) and [NP] (Inset to Figure 3B). The rate constants k_I and k_{II} (Table 3) were calculated from the slopes and intercepts of these linear plots.

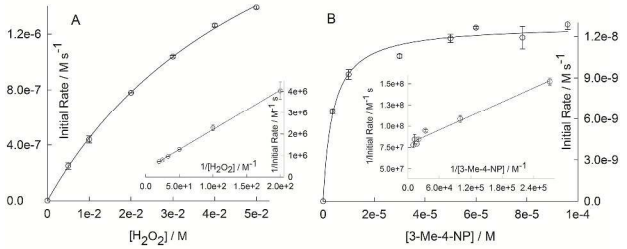

Figure 3 Initial rates of oxidation of 3-Me-4-NP by **1**/H_2O_2 as a function of [H_2O_2] (A) and [3-Me-4-NP] (B). Insets: double reciprocal plots of initial rates as functions of [H_2O_2] (A) and [3-Me-4-NP] (B). Conditions: (A) [3-Me-4-NP] 5×10^{-5} M, [**1**] 5×10^{-7} M; (B) [H_2O_2] 1.25×10^{-3} M, [**1**] 2.4×10^{-7} M; pH 8.4, 25 °C.

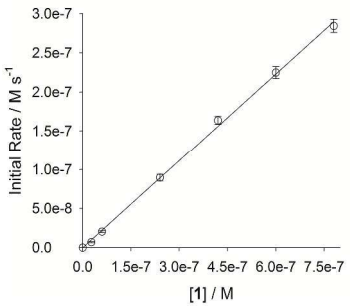

Figure 4 Initial rates of oxidation of 3-Me-4-NP by **1**/H_2O_2 as a function of [**1**]. Conditions: [3-Me-4-NP] 5×10^{-5} M, [H_2O_2] 1.0×10^{-2} M; pH 8.4, 25 °C.

Table 3 Second-Order Rate Constants (k_I and k_{II}, both in M^{-1} s^{-1}) for Oxidation of MNPs by **1**/H_2O_2 at 25 ˚C, pH 8.4 (0.1 M phosphate).

Compounds	H_2O_2 Variation	
	k_I	$k_{II}(\times10^{-4})$
2-Nitrophenol	154±3	[a]
4-Nitrophenol	33±2	1.3±0.3
3-Methyl-4-nitrophenol	90±1	9.5±0.7
2-Methyl-4-nitrophenol	190±10	6.1±0.7
2,6-Dimethyl-4-nitrophenol	2100±100	34±9

[a] could not be reliably measured

The rate constants k_{II} summarized in Table 3 increase in the series 2,6-Me_2-4-NP > 3-Me-4-NP > 2-Me-4-NP > 4-NP, i.e. more electron rich molecules are oxidized faster as might be anticipated. Substituted phenols behave similarly when oxidized by Compound I of horseradish peroxidase (HRP) consistent with the 1*e* oxidation of phenols in the rate-limiting step followed by the loss of a proton to form the phenoxide radical.[38] Interestingly, HRP/H_2O_2 (usually effective for removal of phenols in wastewater treatment[39]) was reported to be inactive towards MNP (2-NP, 3-NP, 4-NP) and 2,6-DNP due to the high reduction potentials of nitrophenols.[40] This fact is consistent with the recalcitrant behaviour of NPs in the environment and reminds the reader that the ultimate powertools that Nature possesses for cleansing the environment of oxidizable contaminants are the oxidizing enzymes of aerobic lifeforms. These findings also demonstrate the virtue of mimicking the oxidizing enzymes with small molecule synthetic catalysts were the reactivity can be controlled by design to give more reactive systems than the enzymes can muster.

The rate constant k_I refers to the interaction between H_2O_2 and **1** and should not depend on the nature of substrate given the mechanism in Scheme 1. However, in the oxidation of MNPs by **1**/H_2O_2 the rate constants k_I actually do vary broadly (60-fold, Table 3) with the nature of MNPs. This behavior signals the likelihood of substrate binding to the catalyst, processes that should mute the catalyst and be subject to steric effects. In fact, there is a systematic decrease in k_I with a decrease in steric crowding around the hydroxyl group of MNPs. The rate constant k_I is the lowest for the least sterically encumbered 4-NP (Table 3), where hydrogen is *ortho* to the OH group and k_I is the highest for 2,6-Me_2-4-NP, where the *ortho* positions are occupied by methyl groups. The k_I value for 2,6-Me_2-4-NP is comparable to that measured for the oxidation of $Fe(CN)_6^{4-}$ to $Fe(CN)_6^{3-}$ by **1**/H_2O_2 (2410±30 M^{-1} s^{-1}, pH 8.4), which proceeds via an outer sphere electron transfer mechanism and can be reasonably considered to be absent of steric effects.[23] The close values of k_I in both cases suggests that the same catalyst species are involved, i.e. that substrate binding to the catalyst in kinetically insignificant for 2,6-Me_2-4-NP. However, the kinetics of oxidation of 4-NP (the MNP with the lowest k_I, Table 3) appeared to be inconsistent with the mechanism in Scheme 1 because the initial rate first increased hyperbolically to reach a maximal value and then decreased sharply with increasing [4-NP] at fixed [**1**] and [H_2O_2] (Figure 5). The combined observations of the variation of k_I, the value of k_I in the expected range for the sterically demanding MNP (2,6-Me_2-4-NP) and the unusual rate profile for 4-NP indicate a change in the mechanism on going from 2,6-Me_2-4-NP to 4-NP.

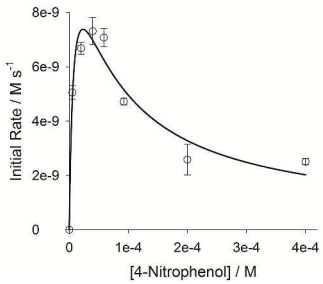

Figure 5 Initial rates of oxidation of 4-NP by **1**/H_2O_2 as a function of [4-NP]. Conditions: [**1**] 1.5×10^{-6} M, [H_2O_2] 1.25×10^{-3} M; pH 8.4, 25 °C. The solid line was calculated using the best fit values of $a_1 - a_4$ (eq 4, Table 4)

A minimalistic mechanism shown in Scheme 2 is sufficient to explain the observed lowering of k_I and the rate inhibition by 4-NP. Its key features are (*i*) the binding of the conjugate base of 4-NP to the Fe^{III} in **1** to form intermediate I_1 (*K*) and (*ii*) activation of H_2O_2 by both Fe^{III} (k_I, k_{-1}) and I_1 (k_{1D}, k_{-1D}) to form identical TAML reactive intermediate (ignoring the possibility that the phenolato ligand may remain bound to "Oxidized TAML"). The mechanism in Scheme 2 leads to eq 3 for the reaction rate, assuming that k_{-I} is negligible,[26] by applying the steady-state approximation to "Oxidized TAML" and using the mass balance equation $[Fe^{III}]_t$ = [Fe^{III}-TAML] + [Oxidized TAML] + [I_1].

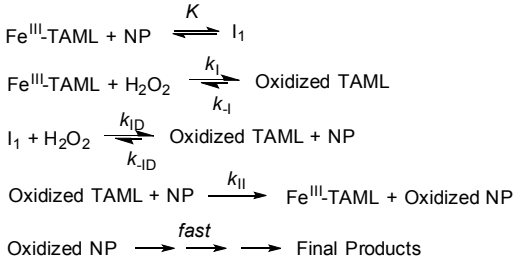

Scheme 2. A minimalistic mechanism for the **1**/H_2O_2 catalyzed oxidative degradation of MNPs which accounts for the experimental variations of k_I with different MNPs and the rate inhibition by 4-NP.

$$Rate = \frac{(k_I[NP]+k_{ID}K[NP]^2)k_{II}[H_2O_2][Fe^{III}]_t}{k_I[H_2O_2]+k_{ID}K[H_2O_2][NP]+(k_{-ID}+k_{II})[NP]+(k_{-ID}+k_{II})K[NP]^2} \quad (3)$$

Equation 3 can be rewritten as eq 4. The parameters $a_1 - a_4$, the meaning of which is shown in Table 4, were calculated by fitting the data in Figure 5 to eq 4 and their values are also shown in Table 4.

$$Rate = \frac{a_1[NP]+a_2[NP]^2}{a_3+a_4[NP]+[NP]^2} \quad (4)$$

Table 4 The effective kinetic parameters for 4-NP oxidation by **1**/H_2O_2 calculated by fitting kinetic data obtained at different concentrations of 4-NP and H_2O_2 to eq 3, respectively, at pH 8.4 and 25 °C.

Effective Parameter	Values of Parameters	Meaning of a_n and b_n parameters in terms of eq 3
a_1 / M^2 s^{-1} [a]	$(8\pm6)\times10^{-13}$	$k_I k_{II}[H_2O_2][Fe^{III}]_t/[(k_{-ID}+k_{II})K]$
a_2 / M s^{-1} [a]	$\sim3\times10^{-10}$	$k_{ID}k_{II}[H_2O_2][Fe^{III}]_t/(k_{-ID}+k_{II})$
a_3 / M^2 [a]	$(5\pm2)\times10^{-10}$	$k_I[H_2O_2]/[(k_{-ID}+k_{II})K]$
a_4 / M [a]	$(6\pm6)\times10^{-5}$	$1/K + k_{ID}[H_2O_2]/(k_{-ID}+k_{II})$
b_1 / M s^{-1} [b]	$(1.6\pm0.1)\times10^{-6}$	$k_{II}[NP][Fe^{III}]_t$
b_2 / M [b]	$(6.2\pm0.9)\times10^{-2}$	$\{(k_{-ID}+k_{II})(1+K[NP])[NP]\}/(k_I+k_{ID}K[NP])$

[a] [**1**] 1.5×10^{-6} M, [H_2O_2] 1.25×10^{-3} M; [b] [**1**] 1.0×10^{-6} M, [4-NP] 1.0×10^{-4} M.

The parameters a_1–a_4 allow us to estimate a value for the rate constant k_{II} of 1.1×10^3 M^{-1} s^{-1} since $k_{II} = a_1/(a_3[Fe^{III}]_t)$. Equation 3 can also be rewritten as eq 5, which prescribes a hyperbolic dependence of the rate on [H_2O_2] (Table 3). The meanings of b_1 and b_2 are shown in Table 4 and their values were calculated by fitting the kinetic data to eq 5. In this case, $k_{II} = b_1/\{[4\text{-NP}][Fe^{III}]_t\} = 1.6\times10^4$ M^{-1} s^{-1} (Table 4), a larger value than that obtained from eq 4. This discrepancy is expected to arise from the potentially oversimplified nature of Scheme 2 when used for interpreting the data in Figure 5 and the uncertainties in estimating the six unknowns, viz. $a_1 - a_4$ and b_1 and b_2. Equations 2 and 5 predict a Michaelis-type dependence on [H_2O_2] so that the calculated k_{II} values so-obtained are close, viz. 1.3×10^4 and 1.6×10^4 M^{-1} s^{-1}, respectively (Table 3). No inhibition by excess of NP was observed for other MNPs (highest [NP] tested ca. 5×10^{-4} M), which is likely due to rather low values of K for 2-Me-4-NP and 3-Me-4-NP. More sterically crowded 2,6-Me_2-4-NP may not bind with **1** at all. Higher concentrations of NPs could not be achieved due their high absorbance.

$$Rate = \frac{b_1[H_2O_2]}{b_2+[H_2O_2]} \quad (5)$$

Supporting evidence for the binding of 4-NP to Fe^{III}-TAML was found from density functional theory (DFT) calculations.[41] Probing the properties of the hypothetical complex {Fe^{III}(TAML)(4-NP)} points to a stable adduct of the nitrophenolate anion and Fe^{III} as shown in Figure 6 with a calculated Fe–O bond distance of 2.06 Å. The energies of all species involved in the complex formation (eq 6) were calculated (see materials and method section for details) to show that the complex formation is energetically favourable.[42]

$$Fe^{III}(TAML)(H_2O) + 4\text{-NP} \rightarrow \{Fe^{III}(TAML)(4\text{-NP})\} \quad (6)$$

The DFT study gives credence to the hypothesis that a stable {Fe^{III}(TAML)(4-NP)} adduct may form in water. The higher concentrations of **1** that were found to be required for the total, degradation of 4-NP (≥99.5%, Table 1) compared to other substituted nitrophenols is also consistent with the inhibition found in the presence of excess of 4-NP. Inhibition of oxidation processes by an excess of substrate has previously been observed for the bleaching by both Fe^{III}-TAML/H_2O_2[43] and [Fe^{III}(octaphenylsulfonato)porphyrazine]/H_2O_2[44] of dyes, Pinacyanol chloride and Orange II, respectively. In both cases, the pre-equilibrium binding of the substrate to Fe^{III} was proposed to account for the observed inhibition.

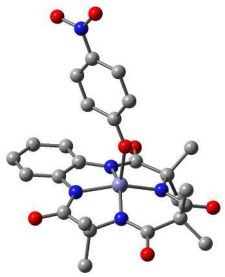

Figure 6 Geometry of the DFT optimized structure of 4-nitrophenol bound to Fe^{III}(TAML). Hydrogen atoms are not shown for clarity. The Fe–O bond distance is 2.06 Å. (Colour code: Fe, lavender; O, red; N, blue; and C, gray)

Dinitrophenol

The rate constants (k_I and k_{II}, Scheme 1, Table 5) associated with the degradation of three DNPs were measured as described above. As with the MNPs, the rate constants k_{II} were found to depend on the electronic properties of the DNPs. 2,5-DNP was oxidized 7 times faster than both 2,6- and 2,4-DNP. The values of k_I obtained for DNPs are shown in Table 5. These rate constants depend on the nature of the substrates and are all much lower than expected (similar to 4-NP).

Table 5 Second-Order Rate Constants (k_I and k_{II}) for Oxidation of DNPs by **1**/H_2O_2 at pH 8 and 25 °C.

Compounds	H_2O_2 Variation	
	k_I	$k_{II}(\times 10^{-4})$
2,4-DNP	9±1	0.2±0.01
2,5-DNP	55±19	1.4±0.3
2,6-DNP	14±1	0.19±0.01

Conclusion

In summary, the present study establishes that **1**/H_2O_2 is an ideal biomimetic catalytic system for the total removal of

persistent mono- and dinitrophenolic pollutants from water under ambient conditions (pH 8, room temperature). The studied nitrophenols were oxidized significantly to nitrogen and carbon minerals rapidly (≤ 45 min), utilizing low catalyst loadings (2×10^{-7}–4×10^{-6} M **1** for 1×10^{-4} M nitrophenol). The toxicity of the starting nitrophenols is substantially reduced and in most cases completely removed (as determined by Microtox® assays) by the **1**/H_2O_2 treatment. The remediation technology described herein requires no special infrastructure and thus should be easy to apply in diverse pollution scenarios. The kinetic, mechanistic and DFT studies of the oxidation mononitrophenols described herein suggest that the substrates bind to the iron(III) in the resting state of the catalyst subject to steric suppression which, when present, manifests as substrate inhibition.

Acknowledgements

T.J.C. thanks the Heinz Endowments for support. S.K. thanks the R. K. Mellon Foundation for a Presidential Fellowship in the Life Sciences (Carnegie Mellon University). A.C. thanks the John and Nancy Harrison for a Legacy Dissertation Fellowship.

Notes and references

[a] Institute for Green Science, Department of Chemistry, Carnegie Mellon University, 4400 5th Avenue, Pittsburgh, PA, USA 15213
ryabov@andrew.cmu.edu
tc1u@andrew.cmu.edu

† Both authors contributed equally to the work

Electronic Supplementary Information (ESI) available: [details of any supplementary information available should be included here]. See DOI: 10.1039/b000000x/

1. A. Chauhan, G. Pandey, N. Sharma, D. Paul, J. Pandey and R. K. Jain, *Environ. Sci. Technol.*, 2010, **44**, 3435-3441.
2. K.-H. Wang, Y.-H. Hsieh, M.-Y. Chou and C.-Y. Chang, *Appl. Catal., B*, 1999, **21**, 1-8.
3. J. Pascal and R. Popovic, *Water Pollution Res. J. Canada.*, 1993, **28**, 687-695.
4. http://www.epa.gov.
5. W. K. Alexander, G. B. Briggs, K. R. Still, W. W. Jederberg, K. MacMahon, W. H. Baker and C. Mackerer, *Appl. Occup. Environ. Hyg.*, 2001, **16**, 487-495.
6. S. Zhao, H. Ma, M. Wang, C. Cao, J. Xiong, Y. Xu and S. Yao, *J. Hazard. Mater.*, 2010, **180**, 86-90.
7. http://www.epa.gov.
8. J. Kiwi, C. Pulgarin and P. Peringer, *Appl. Catal., B*, 1994, **3**, 335-350.
9. C. Li, S. Taneda, A. K. Suzuki, C. Furuta, G. Watanabe and K. Taya, *Toxicol. Appl. Pharmacol.*, 2006, **217**, 1-6.
10. S. J. Yuan, G. P. Sheng, W. W. Li, Z. Q. Lin, R. J. Zeng, Z. H. Tong and H. Q. Yu, *Environ. Sci. Technol.*, 2010, **44**, 5575–5580.
11. C. G. Silva and J. L. Faria, *ChemSusChem*, 2010, **3**, 609-618.
12. P. Gharbani, M. Khosravi, S. M. Tabatabaii, K. Zare, S. Dastmalchi and A. Mehrizad, *Int. J. Environ. Sci. Tech.*, 2010, **7**, 377-384.
13. M. Dua, A. Singh, N. Sethunathan and A. K. Johri, *Appl. Microbiol. Biotechnol.*, 2002, **59**, 143-152.
14. W. S. Chen, C. N. Juan and K. M. Wei, *Chemosphere*, 2005, **60**, 1072-1079.
15. S. Kundu, A. Chanda, L. Espinosa-Marvan, S. K. Khetan and T. J. Collins, *Catal. Sci.Technol.*, 2012, **2**, 1165-1172.
16. S. S. Gupta, M. Stadler, C. A. Noser, A. Ghosh, B. Steinhoff, D. Lenoir, C. P. Horwitz, K.-W. Schramm and T. J. Collins, *Science*, 2002, **296**, 326-328.
17. D. Banerjee, A. L. Markley, T. Yano, A. Ghosh, P. B. Berget, E. G. Minkley, S. K. Khetan and T. J. Collins, *Angew. Chem. Int. Ed.*, 2006, **45**, 3974-3977.
18. A. Chanda, S. K. Khetan, D. Banerjee, A. Ghosh and T. J. Collins, *J. Am. Chem. Soc.* , 2006, **128**, 12058-12059.
19. S. Kundu, A. Chanda, S. K. Khetan, A. D. Ryabov and T. J. Collins, *Environ. Sci. Technol.*, 2013, **47**, 5319-5326.
20. C. P. Horwitz and A. Ghosh, Carnegie Mellon University, PA, USA, 2006 (http://www.chem.cmu.edu/groups/collins/patents/).
21. P. George, *Biochem J.*, 1953, **55**, 220–230.
22. W. L. F. Armarego, C. L. L. Chai, *Purification of Laboratory Chemicals*, 5th ed., Elsevier Science, USA, **2003**
23. S. Kundu, M. Annavajhala, I. V. Kurnikov, A. D. Ryabov and T. J. Collins, *Chem. Eur. J.*, 2012, **18**, 10244 – 10249.
24. D.-L. Popescu, M. Vrabel, A. Brausam, P. Madsen, G. Lente, I. Fabian, A. D. Ryabov, R. v. Eldik and T. J. Collins, *Inorg. Chem.*, 2010, **49**, 11439–11448.
25. A. Ghosh, D. A. Mitchell, A. Chanda, A. D. Ryabov, D. L. Popescu, E. C. Upham, G. J. Collins and T. J. Collins, *J. Am. Chem. Soc.*, 2008, **130**, 15116-15126.
26. N. Chahbane, D.-L. Popescu, D. A. Mitchell, A. Chanda, D. Lenoir, A. D. Ryabov, K.-W. Schramma and T. J. Collins, *Green Chem.*, 2007, **9**, 49–57.
27. P. L. Huston and J. J. Pignatello, *Wat. Res.*, 1999, **33**, 1238-1246.
28. B. Balci, N. Oturan, R. Cherrier and M. A. Oturan, *Wat. Res.*, 2009, **43**, 1924-1934.
29. T. T. Schug, R. Abagyan, B. Blumberg, T. J. Collins, D. Crews, P. L. DeFur, S. M. Dickerson, T. M. Edwards, A. C. Gore, L. J. Guillette, T. Hayes, J. J. Heindel, A. Moores, H. B. Patisaul, T. L. Tal, K. A. Thayer, L. N. Vandenberg, J. C. Warner, C. S. Watson, F. S. v. Saal, R. T. Zoeller, K. P. O'Brien and J. P. Myers, *Green Chem.*, 2013, **15**, 181-198.
30. T. J. Collins and C. Walter, *Sci. Am.*, 2006, **294**, 82-90.
31. A. Chanda, A. D. Ryabov, S. Mondal, L. Alexandrova, A. Ghosh, Y. Hangun-Balkir, C. P. Horwitz and T. J. Collins, *Chem. Eur. J.*, 2006, **12**, 9336-9345.
32. A. Ghosh, A. D. Ryabov, S. M. Mayer, D. C. Horner, D. E. Prasuhn, Jr., S. Sen Gupta, L. Vuocolo, C. Culver, M. P. Hendrich, C. E. F. Rickard, R. E. Norman, C. P. Horwitz and T. J. Collins, *J. Am. Chem. Soc.*, 2003, **125**, 12378-12378.
33. W. C. Ellis, C. T. Tran, R. Roy, M. Rusten, A. Fischer, A. D. Ryabov, B. Blumberg and T. J. Collins, *J. Am. Chem. Soc.*, 2010, **132**, 9774-9781.
34. T. J. Collins, *Acc. Chem. Res.*, 2002, **35**, 782-790.
35. T. J. Collins, *Acc. Chem. Res.*, 1994, **27**, 279-285.

36. S. Kundu, J. V. K. Thompson, A. D. Ryabov and T. J. Collins, *J. Am. Chem. Soc.*, 2011, **133**, 18546–18549.
37. F. Tiago de Oliveira, A. Chanda, D. Banerjee, X. Shan, S. Mondal, L. Que. Jr., E. L. Bominaar, E. Münck and T. J. Collins, *Science*, 2007, **315**, 835–838.
38. D. Job and H. B. Dunford, *Eur. J. Biochem.*, 1976, **66**, 607-614.
39. N. Durán and E. Esposito, *Appl. Catal., B,* 2000, **28**, 83-99.
40. T. Shiga and K. Imaizumi, *Arch. Biochem. Biophys.*, 1975, **167**, 469–479.
41. R. D. Gaussian 03, G. W. T. M. J. Frisch, H. B. Schlegel, G. E. Scuseria, , J. R. C. M. A. Robb, J. A. Montgomery, Jr., T. Vreven, , J. C. B. K. N. Kudin, J. M. Millam, S. S. Iyengar, J. Tomasi, , B. M. V. Barone, M. Cossi, G. Scalmani, N. Rega, , H. N. G. A. Petersson, M. Hada, M. Ehara, K. Toyota, , J. H. R. Fukuda, M. Ishida, T. Nakajima, Y. Honda, O. Kitao, , M. K. H. Nakai, X. Li, J. E. Knox, H. P. Hratchian, J. B. Cross, , C. A. V. Bakken, J. Jaramillo, R. Gomperts, R. E. Stratmann, , A. J. A. O. Yazyev, R. Cammi, C. Pomelli, J. W. Ochterski, , K. M. P. Y. Ayala, G. A. Voth, P. Salvador, J. J. Dannenberg, , S. D. V. G. Zakrzewski, A. D. Daniels, M. C. Strain, , D. K. M. O. Farkas, A. D. Rabuck, K. Raghavachari, , J. V. O. J. B. Foresman, Q. Cui, A. G. Baboul, S. Clifford, , B. B. S. J. Cioslowski, G. Liu, A. Liashenko, P. Piskorz, , R. L. M. I. Komaromi, D. J. Fox, T. Keith, M. A. Al-Laham, , A. N. C. Y. Peng, M. Challacombe, P. M. W. Gill, , W. C. B. Johnson, M. W. Wong, C. Gonzalez, and J. A. Pople, and I. Gaussian, Wallingford CT, 2004., Editon edn.
42. Ground state total energy difference for this system was found to be favourable by 18 kcal mol^{-1}. Although the actual value is not of much relevance as the calibration for such systems is not available, this value gives supportive evidence that such a complex formation is possible. Additional calculations using 2-Me-4-NP and 2,6-diMe-4-NP showed no significant differences in Fe–O bond distance or the binding energy, but progressive changes in binding mode were observed (Figure 3S) that could be attributed to the steric effects of three different NPs. Detailed calculations related to such geometrical changes along with potential electronic changes (e.g. spin state change) were not performed and will be a subject of a separate study.
43. D. A. Mitchell, A. D. Ryabov, S. Kundu, A. Chanda and T. J. Collins, *J. Coord. Chem.*, 2010, **63**, 2605-2618
44. A. Theodoridis, J. Maigut, R. Puchta, E. V. Kudrik and R. v. Eldik, *Inorg. Chem.*, 2008, **47**, 2994-3013.

TOC Figure